

Article

A Facile Route to Fabricate Superhydrophobic Cu₂O Surface for Efficient Oil–Water Separation

Sheng Lei ¹, Xinzuo Fang ¹, Fajun Wang ^{1,2,*}, Mingshan Xue ^{1,2,*} , Junfei Ou ^{1,2}, Changquan Li ¹ and Wen Li ¹

¹ School of Materials Engineering, Jiangsu University of Technology, Changzhou 213001, China; shenglei@jsut.edu.cn (S.L.); fangxz@mail.ustc.edu.cn (X.F.); oujunfei_1982@163.com (J.O.); 70225@nchu.edu.cn (C.L.); 2018500123@jsut.edu.cn (W.L.)

² School of Materials Science and Engineering, Nanchang Hangkong University, Nanchang 330063, China

* Correspondence: jjbxszj@foxmails.com (F.W.); xuems04@mails.uacas.ac.cn (M.X.)

Received: 18 September 2019; Accepted: 11 October 2019; Published: 12 October 2019



Abstract: The mixture of insoluble organics and water seriously affects human health and environmental safety. Therefore, it is important to develop an efficient material to remove oil from water. In this work, we report a superhydrophobic Cu₂O mesh that can effectively separate oil and water. The superhydrophobic Cu₂O surface was fabricated by a facile chemical reaction between copper mesh and hydrogen peroxide solution without any low surface reagents treatment. With the advantages of simple operation, short reaction time, and low cost, the as-synthesized superhydrophobic Cu₂O mesh has excellent oil–water selectivity for many insoluble organic solvents. In addition, it could be reused for oil–water separation with a high separation ability of above 95%, which demonstrated excellent durability and reusability. We expect that this fabrication technique will have great application prospects in the application of oil–water separation.

Keywords: superhydrophobic; Cu₂O; oil–water separation

1. Introduction

Oil in water can reduce the purity of water, and the oily wastewater generated in daily life and industry can also cause serious pollution to the environment [1,2]. Moreover, the presence of water in oil can seriously affect the quality and efficiency of oil such as reducing the service efficiency and life of an engine. Therefore, the research of the separation of the oil–water mixture is of great significance and has broad application prospects. Meanwhile, efficient oil–water separation technology has also attracted great attention [3–7]. In 2004, Jiang et al. prepared a superhydrophobic and superoleophilic coating mesh by spraying polytetrafluoroethylene onto the stainless steel mesh. The contact angles of water and diesel oil on this mesh were 156.2° and 0°, respectively, which realized the effective separation of diesel and water [8]. Inspired by this, many scientists have developed great interest in the application of special wettability materials in oil–water separation.

Over the past decades, researchers have produced a wide variety of materials with superhydrophobic and superoleophilic properties by manipulating and modifying the surface chemical composition and surface roughness. Examples include superhydrophobic metal mesh [9–12], polyurethane sponge [13–15], fiber textile [16–19], metal foam [20,21], polymer membranes [22–24], and so on [25–27], which can selectively repel water from the mixtures of oil and water while allowing oil to penetrate through the materials or to be absorbed, and exhibit high efficiency of oil–water separation performance. However, the preparation process of most of the superhydrophobic materials above-mentioned is complicated and time-consuming, requires special equipment and costly reagents, which severely limits their large-scale production and practical application. Moreover, most

superhydrophobic materials may contaminate oil during oil–water separation due to the use of low surface energy reagents that are not conducive to human health. Therefore, it is reasonably important to develop superhydrophobic oil–water separation materials that are environmentally friendly and without low surface energy reagents.

In this paper, the preparation of a Cu_2O film on copper mesh substrates by a simple one-step chemical reaction method is reported. The as-prepared flower-tufted Cu_2O nanosheet film exhibited superhydrophobicity without modification with low surface energy reagents, as Cu_2O is one of the rare materials that possess a low surface energy and rough structure [28–31]. Water has weak interaction with Cu_2O and does not form bonds on its surface, resulting in the hydrophobicity of Cu_2O . Moreover, the relationship between the reaction time and growth process, morphology, and hydrophobicity of Cu_2O film were investigated. The superhydrophobic Cu_2O mesh also exhibited a superoleophilic property and successfully achieved the separation of various insoluble oil–water mixtures, demonstrating high separation efficiency and reusability. Although Cu_2O formation has been reported by previous papers, a simpler method for preparing superhydrophobic Cu_2O still needs to be developed. Therefore, a method for preparing Cu_2O by reacting copper mesh with hydrogen peroxide is more industrially practical. In addition, the superhydrophobic Cu_2O mesh without similar fluorine-containing reagents is more beneficial to human health, especially for oil–water separation in the production process of edible oils.

2. Materials and Methods

The red copper mesh (purity $\geq 99.97\%$, 200) was purchased from Anping Tairun Wire Mesh Co. Ltd., Hengshui, China. Hydrogen peroxide solution (H_2O_2 , 30 wt % in H_2O), hydrochloric acid, absolute ethyl alcohol, and acetone were bought from Shanghai Chemical Reagent Co. Ltd., Shanghai, China. All chemical reagents used were analytical grade and did not require further processing.

The copper mesh of 30 mm \times 30 mm was ultrasonically cleaned with 0.1 M HCl solution, acetone, and deionized water for 2 min before use, respectively. Then, it was immersed in 100 mL of hydrogen peroxide solution for reaction. After a period of reaction, the copper mesh was taken out and cleaned successively with deionized water and ethanol. Finally, the copper mesh was dried at 120 °C for 5 h under an air atmosphere.

The surface morphology of the copper mesh was determined by a field emission scanning electron microscope (SEM, Sigma 500, Zeiss, Oberkochen, Germany) instrument at 5–15 kV under a vacuum environment. The surface chemical compositions were untreated and the fabricated meshes were measured by a PHI-5702 X-ray photoelectron spectroscopy (XPS, Kratos Analytical Ltd., Manchester, UK). Water contact angle (WCA), oil contact angle (OCA), and water sliding angle (WSA) were measured using an optical contact angle meter (DSA 30, Krüss, Hamburg, Germany) with 5 μL droplets at ambient temperature. The average WCA, OCA, and WSA values were obtained by measuring the same sample in at least five different positions.

3. Results and Discussion

The surface chemical composition of the bare copper mesh and the as-prepared superhydrophobic copper mesh were analyzed in detail using XPS, as depicted in Figure 1. There were three main elements of Cu, O, and C in the XPS survey spectrum of the bare and the superhydrophobic copper mesh surface in Figure 1a. In the high-resolution XPS spectra of the bare copper mesh (Figure 1b), it exhibited two strong peaks centered at 952.4 and 932.6 eV, corresponding to the Cu double peaks of Cu $2p_{1/2}$ and Cu $2p_{3/2}$, respectively [32–35]. Figure 1c shows the photoelectron spectrum of the Cu $2p$ core level for the superhydrophobic copper mesh. Two peaks located at the binding energies of 952.5 and 932.5 eV can be attributed to Cu $2p_{1/2}$ and Cu $2p_{3/2}$, respectively, which agreed well with Cu_2O [36–40]. The O 1s spectrum of the superhydrophobic copper mesh in Figure 1d showed only one peak at 531.1 eV, which can be attributed to Cu_2O [36,39,40]. The above results confirm that the surface of the superhydrophobic copper mesh is mainly Cu_2O . Therefore, it is presumed that hydrogen

peroxide reacts with the copper mesh, leading to the conversion of the upmost layer of Cu to Cu₂O, according to the following reactions:

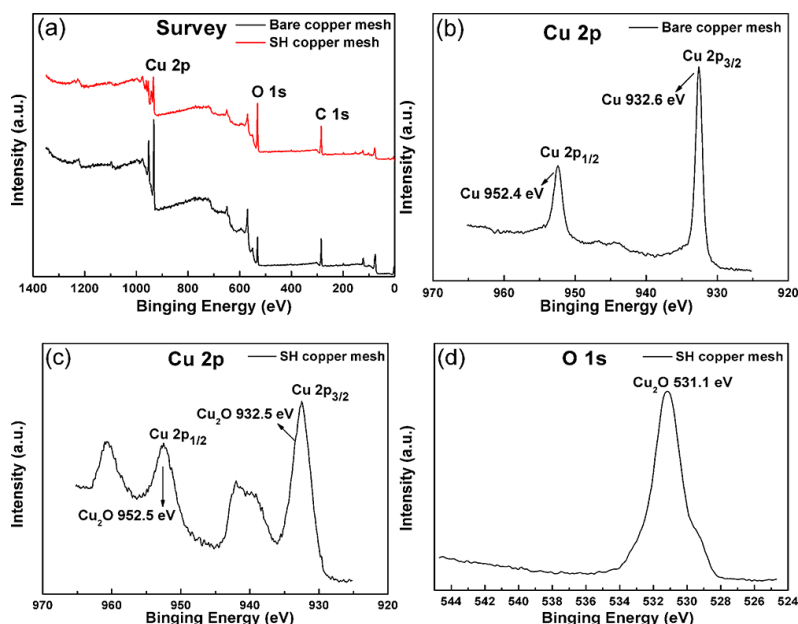


Figure 1. The XPS spectra of the bare and superhydrophobic copper mesh: survey (a), Cu 2p of the bare copper mesh (b), Cu 2p (c) and O 1s (d) of the superhydrophobic copper mesh.

The surface microstructure was considered to be a key factor affecting the surface superhydrophobic properties of the material surface. In the experiment, keeping the concentration and volume of the hydrogen peroxide solution constant, the reaction was carried out by changing the time. The growth process and morphology of the Cu₂O film that changed with reaction time are presented in Figure 2. When the reaction time was 10 min, a large amount of worm-like Cu₂O nanosheets were generated on the surface of the copper mesh (Figure 2a). However, careful observation showed that there were also many Cu₂O nanoparticles presented on the copper mesh surface. After 20 min of reaction, the worm-like nanosheets began to form numerous honeycomb nanosheets. The surface of the copper mesh was mainly covered by honeycomb Cu₂O nanosheet structures and grooves (Figure 2b). After reacting for 30 min, the trend of the growth of the Cu₂O nanosheets became very obvious, as shown in Figure 2c. The surface of the copper mesh was completely covered by a large number of flower-tufted nanosheet structures, which were dense, thin, and relatively uniform in size. Prolonging the reaction time to 40 min, the size of the Cu₂O nanosheets was enlarged and appeared sparse, but the lamellar structure was relatively regular and orderly, as shown in Figure 2d. Increasing the reaction time to 60 min, the Cu₂O nanosheet structure on the surface of the copper mesh showed disorder (Figure 2e). The reason may be that the heat released in the reaction process causes the solution temperature to rise and the reaction to intensify, resulting in corrosion of the partially Cu₂O nanosheet structure. With a further increase of the reaction time to 120 min, the surface of the copper mesh was covered with leaf-like Cu₂O nanosheets, which were thick and uneven in size, as shown in Figure 2f. It is possible that Cu₂O restored the growth of the nanosheet structure due to the decrease in the hydrogen peroxide concentration after a long period of reaction.

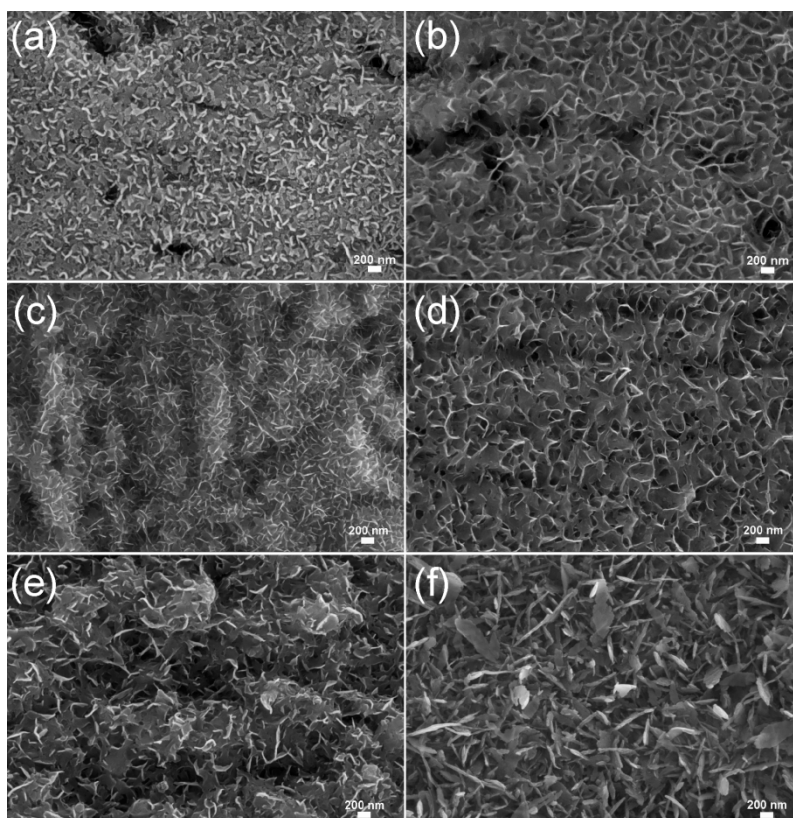


Figure 2. SEM images of the as-prepared Cu₂O surface on copper mesh with different reaction times: (a) 10 min, (b) 20 min, (c) 30 min, (d) 40 min, (e) 60 min, and (f) 120 min.

In order to investigate the effect of the reaction time on wettability, the water contact angles and sliding angles of the Cu₂O surface prepared at different times were detected and are shown in Figure 3. When the reaction time was 10 min, it can be clearly seen that the water contact angle was 148.7° and the sliding angle was 69.8°. When reacted for 20 min, the contact angle reached 157.2°, while the sliding angle was quickly reduced to 17.5°. Prolonging the reaction time to 30 min, the water contact angle and sliding angle were 165.4° and 5.6°, respectively. At this time, the prepared Cu₂O surface exhibited superhydrophobicity. Moreover, when the reaction time increased from 40 to 120 min, the water contact angle and sliding angle of the Cu₂O surface slightly increased and decreased, respectively. This demonstrated that all of the Cu₂O surfaces prepared after 30 min of reaction had good superhydrophobicity and low adhesive hydrophobicity. Therefore, the superhydrophobic Cu₂O surface obtained in 30 min was the best in terms of cost and time. Test results shown in Figure 3 also indicated that the hydrophobic property of the prepared Cu₂O surface increased with the extension of reaction time. On the one hand, the amount of Cu₂O increased with the reaction time, which gradually covered the surface of the copper mesh and reduced its surface energy. On the other hand, the Cu₂O nanosheet structures of the copper mesh surface changed with the reaction time, and the corresponding morphology is shown in Figure 2. These micro/nano-rough structures contribute to reduce the surface contact area with water droplets.

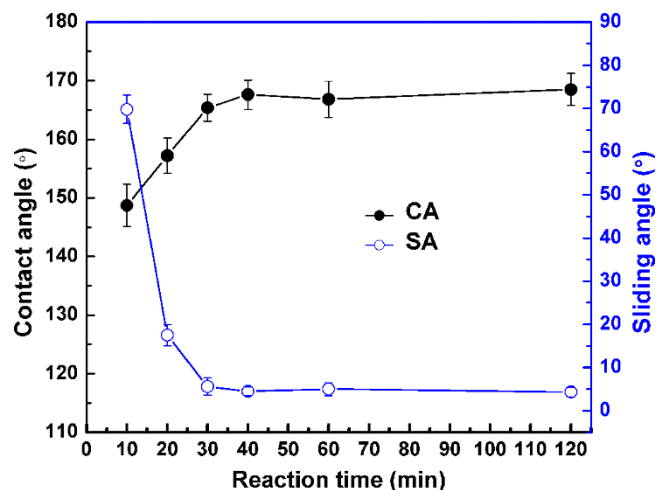


Figure 3. Water contact angles and sliding angles of the as-prepared Cu₂O surface with different reaction times.

Figure 4 displays the surface morphology and water wetting properties of the bare copper mesh and superhydrophobic Cu₂O mesh. As illustrated in Figure 4a, the surface of the bare copper mesh was smooth, which could be clearly observed even in the SEM image at higher magnification (Figure 4b). The contact angle of the water droplets on the surface of the copper mesh was 119.8°, but the water droplets did not drop when rotated 90°. In addition, the contact angle of organic solvents such as toluene, trichloromethane, gasoline, and kerosene on the surface of the bare copper mesh was close to 0°. As evidenced from Figure 4c, the superhydrophobic Cu₂O mesh surface was very rough, which was prepared by reacting for 30 min. In the high-magnification SEM image, many flower-tufted Cu₂O nanosheets were observed on the surface of the copper mesh (Figure 4d). The contact angle of the water droplets on the surface of the superhydrophobic Cu₂O mesh reached 165.4°, and the sliding angle was as low as 5.6°. However, the contact angle of toluene, trichloromethane, and other oils in the superhydrophobic Cu₂O mesh was approximately 0°, which confirmed that the prepared superhydrophobic Cu₂O mesh also had excellent superoleophilicity. The pore size of the copper mesh was about 75 μm, and the hierarchical micro/nanostructure was constructed by combining the flower-tufted Cu₂O nanosheets on the surface. The grooves and gaps created by these rough structures can capture a large volume of air, resulting in large water contact angles and small sliding angles on the surface, which can be explained by the Cassie–Baxter equation [41]:

$$\cos \theta_r = f_1 \cos \theta - f_2 \quad (2)$$

where θ_r is the contact angle of liquid on the rough surface; θ is the contact angle of liquid on the corresponding smooth surface; f_1 is the proportion of the solid surface actually in contact with liquid; f_2 is the proportion of air trapped in the hole in contact with liquid; and $f_1 + f_2 = 1$. The water contact angles on the rough superhydrophobic Cu₂O mesh and the smooth copper mesh were 165.4° and 119.8°, respectively. Therefore, the f_2 of the superhydrophobic Cu₂O mesh calculated by Equation (2) was 0.936, indicating that the contact area between water and air accounted for up to 93.6%. Correspondingly, the contact between water and solid surface only accounts for 6.4%, which is similar to the results reported by Karapanagiotis et al. [42]. The small water-solid contact area demonstrates the good superhydrophobic property on the surface.

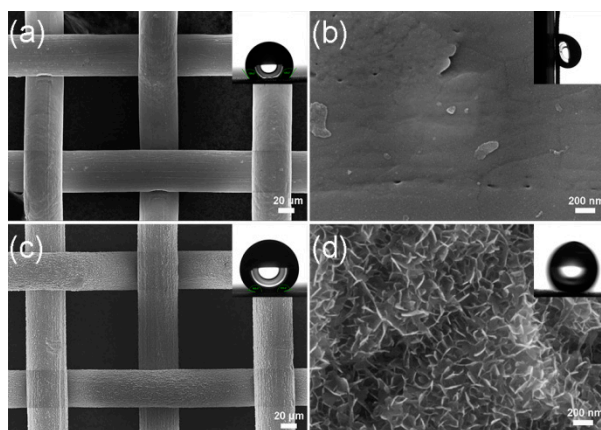


Figure 4. SEM images of the surfaces of bare (a,b) and superhydrophobic Cu₂O mesh (c,d). The insets show the optical images of the water contact angle and sliding angle.

The oil–water separation property of the as-prepared superhydrophobic Cu₂O mesh was investigated with a self-made device, as shown in Figure 5. The filter was made of superhydrophobic Cu₂O mesh sandwiched between the upper glass cylinder and the lower funnel. The superhydrophobic mesh had a thickness of 0.1 mm and was firmly fixed, so that water did not leak from the contact surface. The effective filter diameter of the filter device was 20 mm. When a drop of toluene dyed with oil red O contacted the surface of the superhydrophobic Cu₂O mesh, it spread rapidly and penetrated the mesh, leaving only red marks on the underlying filter paper. However, the water droplet remained spherical on the surface of the superhydrophobic Cu₂O mesh (Figure 5a). A total of 10 mL toluene and 10 mL water dyed with methylene blue were mixed into a 20 mL insoluble oil–water mixture (Figure 5b). As the oil–water mixture was slowly injected into the separation device, the oil easily passed through the superhydrophobic Cu₂O mesh into the beaker under the action of gravity (Figure 5c). After the oil–water separation was completed, the oil was collected in the beaker while the water was kept in the container on the superhydrophobic Cu₂O mesh (Figure 5d). The same separation process was also applicable to the mixture of water and other oils such as gasoline, kerosene, trichloromethane, hexane, edible oil, and so on. In addition, the oil flux of the superhydrophobic Cu₂O mesh was measured and the values were calculated by the following equation:

$$J = V/St \quad (3)$$

where V is the volume of oil is 0.01 L; S is the effective oil-passing area of the superhydrophobic Cu₂O mesh; and t is the time for the permeation of 0.01 L of oil. As a result, the flux values of toluene, gasoline, kerosene, trichloromethane, hexane, and edible oil of the superhydrophobic Cu₂O mesh were 8.18, 7.68, 7.72, 8.36, 8.12, and 0.53 L·m⁻²·s⁻¹, respectively. The viscosity of edible oil was larger than that of other oils, which led to a long time required to penetrate the copper mesh, and the flux value was small.

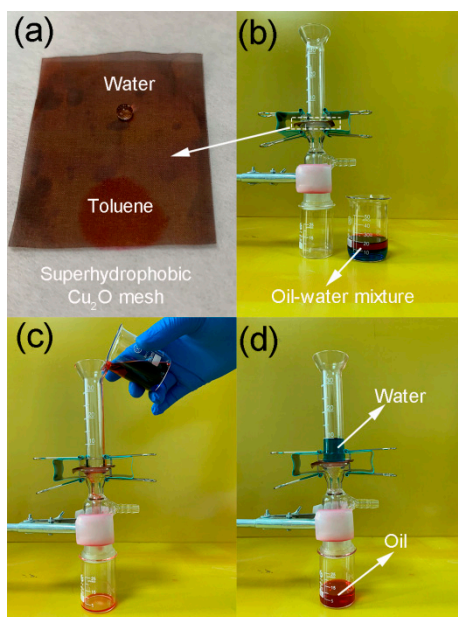


Figure 5. (a) Water and oil on the surface of the superhydrophobic Cu₂O mesh, (b) separation device and oil–water mixture (toluene was dyed with oil red O and water was dyed with methylene blue), (c,d) oil–water separation process.

The oil–water separation performance was investigated using the as-prepared superhydrophobic Cu₂O mesh. The oil–water separation efficiency of the superhydrophobic Cu₂O mesh was evaluated and analyzed by the following formula:

$$\eta = V/V_0 \times 100\% \quad (4)$$

where η represents the separation efficiency and V and V_0 are the oil volume before and after the separation experiment, respectively [43,44]. Figure 6a shows the separation efficiency of several different types of oil and water mixtures. It can be clearly seen that the initial separation efficiency of trichloromethane, toluene, gasoline, kerosene, hexane, and edible oil all exceeded 95%. The relatively low separation efficiency of edible oil was mainly due to its high viscosity, which was slightly stuck to the container wall and mesh surface during the oil–water separation process. More importantly, the superhydrophobic Cu₂O mesh exhibited excellent reusability. As illustrated in Figure 6b, the oil–water separation efficiency was still as high as 96.9% after 50 cycles of repeated separation test of the toluene and water mixture. The slight decrease in the oil–water separation efficiency could be attributed to the volatilization and loss of toluene in the test process. In addition, the superhydrophobic Cu₂O mesh had the same superhydrophobicity and superoleophilicity after washing and drying, indicating its good potential application prospects in oil–water separation.

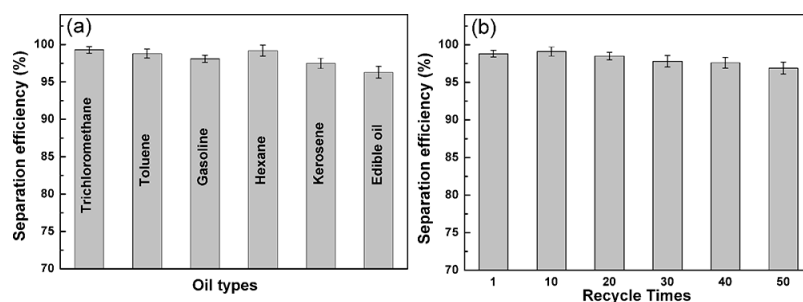


Figure 6. Oil separation efficiency of the superhydrophobic Cu₂O mesh: (a) for various oil–water mixtures in the first cycle, (b) for toluene after different separation cycles.

4. Conclusions

In summary, the superhydrophobic Cu₂O mesh was prepared by a one-step reaction of red copper mesh and hydrogen peroxide without modification of any low surface energy reagent. The growth process, morphology, and hydrophobicity of the Cu₂O film changed with the increase in reaction time. The superhydrophobic and superoleophilic Cu₂O mesh with the flower-tufted nanosheet structures was obtained at an optimum reaction time of 30 min, and the water contact angle, sliding angle, and oil contact angle were 165.4°, 5.6°, and 0°, respectively. Moreover, the as-prepared superhydrophobic Cu₂O mesh could separate various insoluble oil–water mixtures, and the oil–water separation efficiency was more than 95%. In addition, the superhydrophobic Cu₂O mesh displayed good reusability and stability after 50 oil–water separation cycles. This simple, low-cost, large-area preparation technique for superhydrophobic Cu₂O mesh will have a wide application prospect in the field of oil–water separation.

Author Contributions: Conceptualization, S.L.; Methodology, S.L.; Resources, S.L., F.W., and M.X.; Validation, X.F., M.X., and J.O.; Investigation, S.L., X.F., and J.O.; Data curation, S.L.; Writing-Original Draft Preparation, S.L.; Writing-Review and Editing, S.L., F.W., and M.X.; Supervision, C.L.; Project Administration, S.L.; Funding Acquisition, M.X. and W.L.

Funding: The work was supported by the National Natural Science Foundation of China (Nos. 51662032 and 11864024), the Natural Science Foundation of Department of Science and Technology of Jiangsu Province (No. BK20191478), the Innovative and Entrepreneurial Talent Plan of Jiangsu Province, and the Qing Lan Project of Jiangsu Province.

Conflicts of Interest: The authors declare no conflicts of interest.

References

1. Ahmed, A.F.; Ahmad, J.; Basma, Y.; Ramzi, T. Assessment of alternative management techniques of tank bottom petroleum sludge in Oman. *J. Hazard. Mater.* **2007**, *141*, 557–564.
2. Guterman, L. Exxon valdez turns 20. *Science* **2009**, *323*, 1558–1559. [[CrossRef](#)] [[PubMed](#)]
3. Chen, G.H.; He, G.H. Separation of water and oil from water-in-oil emulsion by freeze/thaw method. *Sep. Purif. Technol.* **2003**, *31*, 83–89. [[CrossRef](#)]
4. Mullin, J.V.; Champ, M.A. Introduction/overview to in situ burning of oil spills. *Spill Sci. Technol. Bull.* **2003**, *8*, 323–330. [[CrossRef](#)]
5. Zouboulis, A.I.; Avranas, A. Treatment of oil-in-water emulsions by coagulation and dissolved-air flotation. *Colloid. Surface A* **2000**, *172*, 153–161. [[CrossRef](#)]
6. Adebajo, M.O.; Frost, R.L.; Kloprogge, J.T.; Carmody, O.; Kokot, S. Porous materials for oil spill cleanup: a review of synthesis and absorbing properties. *J. Porous Mater.* **2003**, *10*, 159–170. [[CrossRef](#)]
7. Nyankson, E.; Olasehinde, O.; John, V.T.; Gupta, R.B. Surfactant-loaded halloysite clay nanotube dispersants for crude oil spill remediation. *Ind. Eng. Chem. Res.* **2015**, *54*, 9328–9341. [[CrossRef](#)]
8. Feng, L.; Zhang, Z.Y.; Mai, Z.H.; Ma, Y.M.; Liu, B.Q.; Jiang, L.; Zhu, D.B. A super-hydrophobic and super-oleophilic coating mesh film for the separation of oil and water. *Angew. Chem. Int. Ed.* **2004**, *43*, 2012–2014. [[CrossRef](#)]
9. Gao, Y.F.; Cheng, M.J.; Wang, B.L.; Feng, Z.G.; Shi, F. Diving-surfacing cycle within a stimulus-responsive smart device towards developing functionally cooperating systems. *Adv. Mater.* **2010**, *22*, 5125–5128. [[CrossRef](#)]
10. Pan, Q.M.; Wang, M. Miniature boats with striking loading capacity fabricated from superhydrophobic copper meshes. *ACS Appl. Mater. Inter.* **2009**, *1*, 420–423. [[CrossRef](#)]
11. Jiang, Z.X.; Geng, L.; Huan, Y.D. Design and fabrication of hydrophobic copper mesh with striking loading capacity and pressure resistance. *J. Phys. Chem. C* **2010**, *114*, 9370–9378. [[CrossRef](#)]
12. Tian, D.L.; Zhang, X.F.; Zhai, J.; Jiang, L. Photocontrollable water permeation on the micro/nanoscale hierarchical structured ZnO mesh films. *Langmuir* **2011**, *27*, 4265–4270. [[CrossRef](#)] [[PubMed](#)]
13. Zhu, Q.; Pan, Q.M.; Liu, F.T. Facile removal and collection of oils from water surfaces through superhydrophobic and superoleophilic sponges. *J. Phys. Chem. C* **2011**, *115*, 17464–17470. [[CrossRef](#)]
14. Zhou, X.Y.; Zhang, Z.Z.; Xu, X.H.; Men, X.H.; Zhu, X.T. Facile fabrication of superhydrophobic sponge with selective absorption and collection of oil from water. *Ind. Eng. Chem. Res.* **2013**, *52*, 9411–9416. [[CrossRef](#)]

15. Wang, C.F.; Lin, S.J. Robust superhydrophobic/superoleophilic sponge for effective continuous absorption and expulsion of oil pollutants from water. *ACS Appl. Mater. Inter.* **2013**, *5*, 8861–8864. [[CrossRef](#)]
16. Li, S.H.; Huang, J.Y.; Chen, Z.; Chen, G.Q.; Lai, Y.K. A review on special wettability textiles: theoretical models, fabrication technologies and multifunctional applications. *J. Mater. Chem. A* **2017**, *5*, 31–55. [[CrossRef](#)]
17. Xu, Z.G.; Zhao, Y.; Wang, H.X.; Zhou, H.; Qin, C.X.; Wang, X.G.; Lin, T. Fluorine-free superhydrophobic coatings with pH-induced wettability transition for controllable oil-water separation. *ACS Appl. Mater. Inter.* **2016**, *8*, 5661–5667. [[CrossRef](#)]
18. Zhang, M.; Li, J.; Zang, D.L.; Lu, Y.; Gao, Z.X.; Shi, J.Y.; Wang, C.Y. Preparation and characterization of cotton fabric with potential use in UV resistance and oil reclaim. *Carbohydr. Polym.* **2016**, *137*, 264–270. [[CrossRef](#)]
19. Ou, J.F.; Wan, B.B.; Wang, F.J.; Xue, M.S.; Wu, H.M.; Li, W. Superhydrophobic fibers from cigarette filters for oil spill cleanup. *RSC Adv.* **2016**, *6*, 44469–44474. [[CrossRef](#)]
20. Cheng, M.J.; Gao, Y.F.; Guo, X.P.; Shi, Z.Y.; Chen, J.F.; Shi, F. A functionally integrated device for effective and facile oil spill cleanup. *Langmuir* **2011**, *27*, 7371–7375. [[CrossRef](#)]
21. Jin, X.; Shi, B.R.; Zheng, L.C.; Pei, X.H.; Zhang, X.Y.; Sun, Z.Q.; Du, Y.; Kim, J.H.; Wang, X.L.; Dou, S.X.; et al. Bio-inspired multifunctional metallic foams through the fusion of different biological solutions. *Adv. Funct. Mater.* **2014**, *24*, 2721–2726. [[CrossRef](#)]
22. Zhang, W.; Shi, Z.; Zhang, F.; Liu, X.; Jin, J.; Jiang, L. Superhydrophobic and superoleophilic PVDF membranes for effective separation of water-in-oil emulsions with high flux. *Adv. Mater.* **2013**, *25*, 2071–2076. [[CrossRef](#)] [[PubMed](#)]
23. Huang, M.L.; Si, Y.; Tang, X.M.; Zhu, Z.G.; Ding, B.; Liu, L.F.; Zheng, G.; Luo, W.J.; Yu, J.Y. Gravity driven separation of emulsified oil-water mixtures utilizing in situ polymerized superhydrophobic and superoleophilic nanofibrous membranes. *J. Mater. Chem. A* **2013**, *1*, 14071–14074. [[CrossRef](#)]
24. Fang, W.; Liu, L.; Li, T.; Dang, Z.; Qiao, C.; Xu, J.; Wang, Y. Electrospun N-substituted polyurethane membranes with self-healing ability for self-cleaning and oil/water separation. *Chemistry* **2016**, *22*, 878–883. [[CrossRef](#)]
25. Gui, X.C.; Wei, J.Q.; Wang, K.L.; Cao, A.Y.; Zhu, H.W.; Jia, Y.; Shu, Q.K.; Wu, D.H. Carbon nanotube sponges. *Adv. Mater.* **2010**, *22*, 617–621. [[CrossRef](#)]
26. Wei, Y.B.; Qi, H.; Gong, X.; Zhao, S.F. Specially wettable membranes for oil-water separation. *Adv. Mater. Inter.* **2018**, 1800576. [[CrossRef](#)]
27. Yang, Y.; Tong, Z.; Ngai, T.; Wang, C.Y. Nitrogen-rich and fire-resistant carbon aerogels for the removal of oil contaminants from water. *ACS Appl. Mater. Inter.* **2014**, *6*, 6351–6360. [[CrossRef](#)]
28. Song, W.; Zhang, J.J.; Xie, Y.F.; Cong, Q.; Zhao, B. Large-area unmodified superhydrophobic copper substrate can be prepared by an electroless replacement deposition. *J. Colloid Interface Sci.* **2009**, *329*, 208–211. [[CrossRef](#)]
29. Chang, F.M.; Cheng, S.L.; Hong, S.J.; Sheng, Y.J.; Tsao, H.K. Superhydrophilicity to superhydrophobicity transition of CuO nanowire films. *Appl. Phys. Lett.* **2010**, *96*, 114101. [[CrossRef](#)]
30. Wang, F.J.; Lei, S.; Xue, M.S.; Ou, J.F.; Li, W. In Situ separation and collection of oil from water surface via a novel superoleophilic and superhydrophobic oil containment boom. *Langmuir* **2014**, *30*, 1281–1289. [[CrossRef](#)]
31. Ding, Y.B.; Li, Y.; Yang, L.L.; Li, Z.Y.; Xin, W.H.; Liu, X.; Pan, L.; Zhao, J.P. The fabrication of controlled coral-like Cu₂O films and their hydrophobic property. *Appl. Surf. Sci.* **2013**, *266*, 395–399. [[CrossRef](#)]
32. Singh, V.; Sheng, Y.J.; Tsao, H.K. Facile fabrication of superhydrophobic copper mesh for oil/water separation and theoretical principle for separation design. *J. Taiwan Inst. Chem. E* **2018**, *87*, 1–8. [[CrossRef](#)]
33. Monte, M.; Munuera, G.; Costa, D.; Conesa, J.C.; Martinez, A.A. Near-ambient XPS characterization of interfacial copper species in ceria-supported copper catalysts. *Phys. Chem. Chem. Phys.* **2015**, *17*, 29995–30004. [[CrossRef](#)] [[PubMed](#)]
34. Li, B.; Luo, X.; Zhu, Y.; Wang, X. Immobilization of Cu(II) in KIT-6 supported Co₃O₄ and catalytic performance for epoxidation of styrene. *App. Surf. Sci.* **2015**, *359*, 609–620. [[CrossRef](#)]
35. Embden, J.V.; Tachibana, Y. Synthesis and characterisation of famatinite copper antimony sulfide nanocrystals. *J. Mater. Chem.* **2012**, *22*, 11466–11469. [[CrossRef](#)]
36. Lv, Y.Q.; Shi, B.Z.; Qi, Y.; Su, X.F.; Liu, L.; Tian, L.H.; Ding, J. Synthesis and characterization of the maize-leaf like Cu₂O nanosheets array film via an anodic oxidation method. *J. Alloy. Compd.* **2019**, *773*, 706–712. [[CrossRef](#)]

37. Cheng, Z.P.; Xu, J.M.; Zhong, H.; Chu, X.Z.; Song, J. Repeatable synthesis of Cu₂O nanorods by a simple and novel reduction route. *Mater. Lett.* **2011**, *65*, 1871–1874. [[CrossRef](#)]
38. Zhou, C.L.; Cheng, J.; Hou, K.; Zhu, Z.T.; Zheng, Y.F. Preparation of CuWO₄@Cu₂O film on copper mesh by anodization for oil/water separation and aqueous pollutant degradation. *Chem. Eng. J.* **2017**, *307*, 803–811. [[CrossRef](#)]
39. Ai, Z.H.; Zhang, L.Z.; Lee, S.C.; Ho, W.K. Interfacial hydrothermal synthesis of Cu@Cu₂O core-shell microspheres with enhanced visible-light-driven photocatalytic activity. *J. Phys. Chem. C* **2009**, *113*, 20896–20902. [[CrossRef](#)]
40. Platzman, I.; Brener, R.; Haick, H.; Tannenbaum, R. Oxidation of polycrystalline copper thin films at ambient conditions. *J. Phys. Chem. C* **2008**, *112*, 1101–1108. [[CrossRef](#)]
41. Cassie, A.B.D.; Baxter, S. Wettability of porous surfaces. *Trans. Faraday Soc.* **1944**, *40*, 546–551. [[CrossRef](#)]
42. Manoudis, P.N.; Karapanagiotis, I. Modification of the wettability of polymer surfaces using nanoparticles. *Prog. Org. Coat.* **2014**, *77*, 331–338. [[CrossRef](#)]
43. Lu, Y.; Sathasivam, S.; Song, J.; Chen, F.; Xu, W.; Carmalt, C.J.; Parkin, I.P. Creating superhydrophobic mild steel surfaces for water proofing and oil-water separation. *J. Mater. Chem. A* **2014**, *2*, 11628–11634. [[CrossRef](#)]
44. Li, J.; Yan, L.; Li, H.; Li, W.; Zha, F.; Lei, Z. Underwater superoleophobic palygorskite coated meshes for efficient oil/water separation. *J. Mater. Chem. A* **2015**, *3*, 14696–14702. [[CrossRef](#)]



© 2019 by the authors. Licensee MDPI, Basel, Switzerland. This article is an open access article distributed under the terms and conditions of the Creative Commons Attribution (CC BY) license (<http://creativecommons.org/licenses/by/4.0/>).